

TBI CONTUSION SEGMENTATION FROM MRI USING CONVOLUTIONAL NEURAL NETWORKS

Snehashis Roy^a * John A. Butman^b Leighton Chan^c Dzung L. Pham^a

^a Center for Neuroscience and Regenerative Medicine, Henry Jackson Foundation

^b Radiology and Imaging Sciences, Clinical Center, National Institute of Health

^c Rehabilitation Medicine Department, National Institute of Health

ABSTRACT

Traumatic brain injury (TBI) is caused by a sudden trauma to the head that may result in hematomas and contusions and can lead to stroke or chronic disability. An accurate quantification of the lesion volumes and their locations is essential to understand the pathophysiology of TBI and its progression. In this paper, we propose a fully convolutional neural network (CNN) model to segment contusions and lesions from brain magnetic resonance (MR) images of patients with TBI. The CNN architecture proposed here was based on a state of the art CNN architecture from Google, called Inception. Using a 3-layer Inception network, lesions are segmented from multi-contrast MR images. When compared with two recent TBI lesion segmentation methods, one based on CNN (called DeepMedic) and another based on random forests, the proposed algorithm showed improved segmentation accuracy on images of 18 patients with mild to severe TBI. Using a leave-one-out cross validation, the proposed model achieved a median Dice of 0.75, which was significantly better ($p < 0.01$) than the two competing methods.

Index Terms— TBI, convolutional neural network, segmentation, lesions, deep learning

1. INTRODUCTION

Accurate segmentation of contusions, edema, hemorrhages, and lesions is important for understanding the effects of traumatic brain injury (TBI). Although the exact pathophysiology of TBI is unknown, TBI lesions have been shown to be associated with cognitive decline [1] and other neurological impairments [2]. Quantitative information about types, locations, and volumes of the lesions can be correlated with the patient outcome and mortality [3] to better identify patients at risk for poor outcomes. The presence of TBI is typically assessed from CT images in a clinical setting. MR images provide details of TBI lesions that are not easily observed on

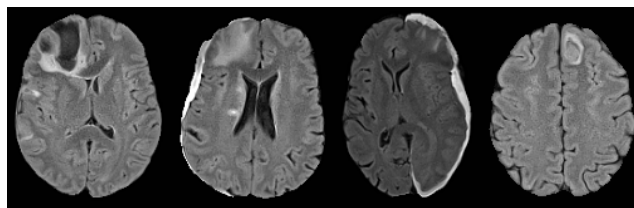


Fig. 1. Examples of hemorrhages are shown on FLAIR images for 4 patients with TBI.

CT because MR images have higher resolution and better soft tissue contrast. Therefore segmentation of TBI lesions from magnetic resonance imaging (MRI) may provide valuable insights into the understanding of TBI.

Many machine learning algorithms have been proposed for segmenting lesions from MR images from patients with multiple sclerosis (MS) and Alzheimer’s disease (AD). However, TBI contusions and lesions are more heterogeneous compared to MS or AD, making automated segmentation a challenging task. An example of different types of TBI lesions are shown in Fig. 1. Clearly, there is considerable variability of the lesions in terms of shape, size, location, and overall intensity distribution. Instead of segmenting different parts of the lesions, such as encephalomalacia or blood, we propose to label all the abnormal tissue in a binary classification.

Most of the previously successful lesion segmentation methods are supervised; training data are derived from manual lesion delineations on multi-contrast MR images, and machine learning algorithms, such as random forest [5, 6], are used to learn a mapping between intensities and lesion labels. In atlas based methods, multiple normal atlases are registered to a subject brain with pathologies to detect voxels with out-of-atlas intensity distributions [7], which correspond to pathological regions. Similarly, label fusion type techniques use tissue priors from normal atlases to detect voxels with pathological intensities and segment whole brain [8]. Dictionary learning has also been applied for lesion segmentation where image patch dictionaries are learnt for patches

*This work was supported by the Department of Defense in the Center for Neuroscience and Regenerative Medicine and the Intramural Research Program of the National Institutes of Health. This work was also partially supported by grant from National MS Society RG-1507-05243.

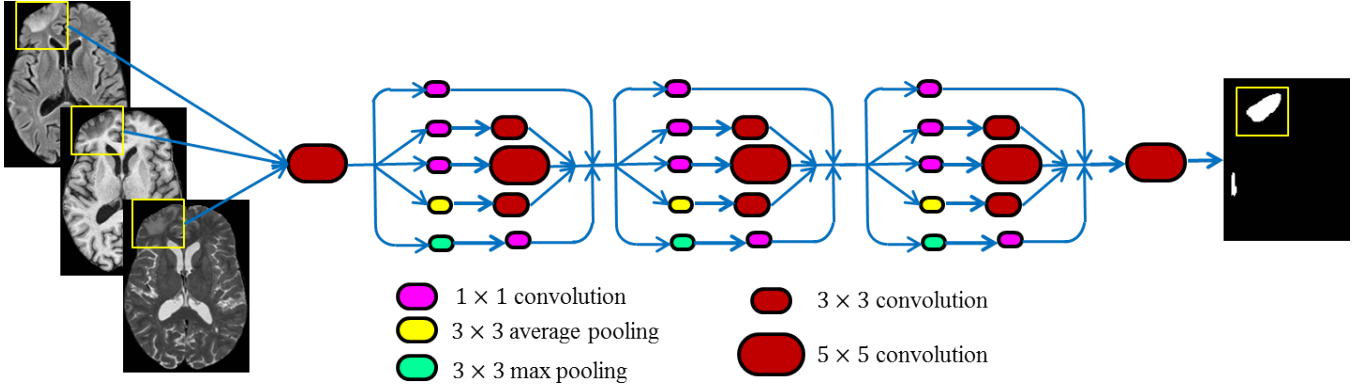


Fig. 2. The proposed CNN architecture using modified Google Inception [4] block is shown. Patches from MPRAGE, T_2 -w and FLAIR images are passed through 3 modified Inception blocks, the output being a patch of lesion memberships.

containing normal tissues and lesions [9, 10].

Recently, convolutional neural networks (CNNs), or deep learning [11], have been successful in tumor and stroke lesion segmentation [12]. Unlike traditional machine learning methods, CNNs do not need hand crafted features, which make them applicable to diverse problems. In recent tumor segmentation challenges [12], the top rated methods have used neural networks. These methods employ either 2D [13, 14] or 3D [15] image patches containing normal tissues as well as lesion voxels, and dense networks were trained using manual delineations of lesions. CNNs have the advantage of being fast because they are implemented in GPUs; segmentation of a subject brain can be completed in only couple minutes [15].

In this paper, we propose an automated TBI lesion segmentation method using CNNs. We explored a recent state-of-the-art network architecture called Inception [4], initially proposed to classify natural images by Google, to segment lesions using multi-contrast MR images. We compared this method with a random forest based method [5] as well as another recent CNN based method DeepMedic [15] to show that the proposed method produced improved segmentation performance.

2. DATASET

The proposed segmentation was evaluated on multi-contrast images of 18 patients with mild to severe TBI. MPRAGE, T_2 -w, and FLAIR images were acquired on a Siemens 3T scanners. The imaging parameters were as follows, MPRAGE: $T_R = 2530\text{ms}$, $T_E = 3.03\text{ms}$, $T_I = 1100\text{ms}$, flip angle 7° , resolution $1 \times 1 \times 1 \text{ mm}^3$, size $256 \times 256 \times 176$; T_2 : $T_R = 3200\text{ms}$, $T_E = 409\text{ms}$, flip angle 120° , resolution $0.98 \times 0.98 \times 1 \text{ mm}^3$, size $512 \times 512 \times 176$; FLAIR: $T_R = 9.09\text{s}$, $T_E = 112\text{ms}$, $T_I = 2450\text{ms}$, flip angle 120° , resolution $0.86 \times 0.86 \times 3 \text{ mm}^3$, size $256 \times 256 \times 50$. FLAIR and T_2 -w images were rigidly registered [16] to the MPRAGE. Then for every subject, the MPRAGE was stripped [17] and

the same brainmask was applied to the other contrasts. All of the stripped images were corrected for any intensity inhomogeneity [18]. Finally TBI lesions were manually delineated on the registered FLAIR to serve as training and evaluation data. The manual segmentations were also examined by a neuroradiologist for accuracy.

3. METHOD

The proposed fully convolutional network architecture is shown in Fig. 2. The network used cascades of 3 modified Inception modules [4]. Each module consisted of parallel layers of convolutions, max-pooling, and average pooling. Each convolution was followed by a rectified linear unit (ReLU), which clamped any non-zero element in the convolution output to zero. Max-pooling and average pooling involve choosing a maximum value or average value over a sliding window of pre-defined size. The original Inception module, as proposed in [4], consisted of 4 parallel pathways, three 1×1 convolutions and a max-pooling layer. We modified this architecture by adding another parallel pathway with an average pooling layer (yellow boxes in Fig. 2) followed by 3×3 convolutions (see Fig. 2). The rationale behind adding this extra layer arose from the visual representation of the lesions, shown in Fig. 1. Lesions in TBI can have different intensity profiles, both bright and dark depending on the time between the injury and the scan. To detect these intensities, average pooling acts as a low resolution feature map without actually having to downsample the image. This can have some practical implications which are explained later. The number of filters for each convolution was kept the same as the original paper [4], with 32 average pooling filters in each modified Inception module.

In recent famous CNN architectures such as ZFNet [19] or VGGNet [20], convolutions and pooling were used in a serial manner and fully connected (or dense) layers were added at the end of the networks for classification purpose. As a conse-

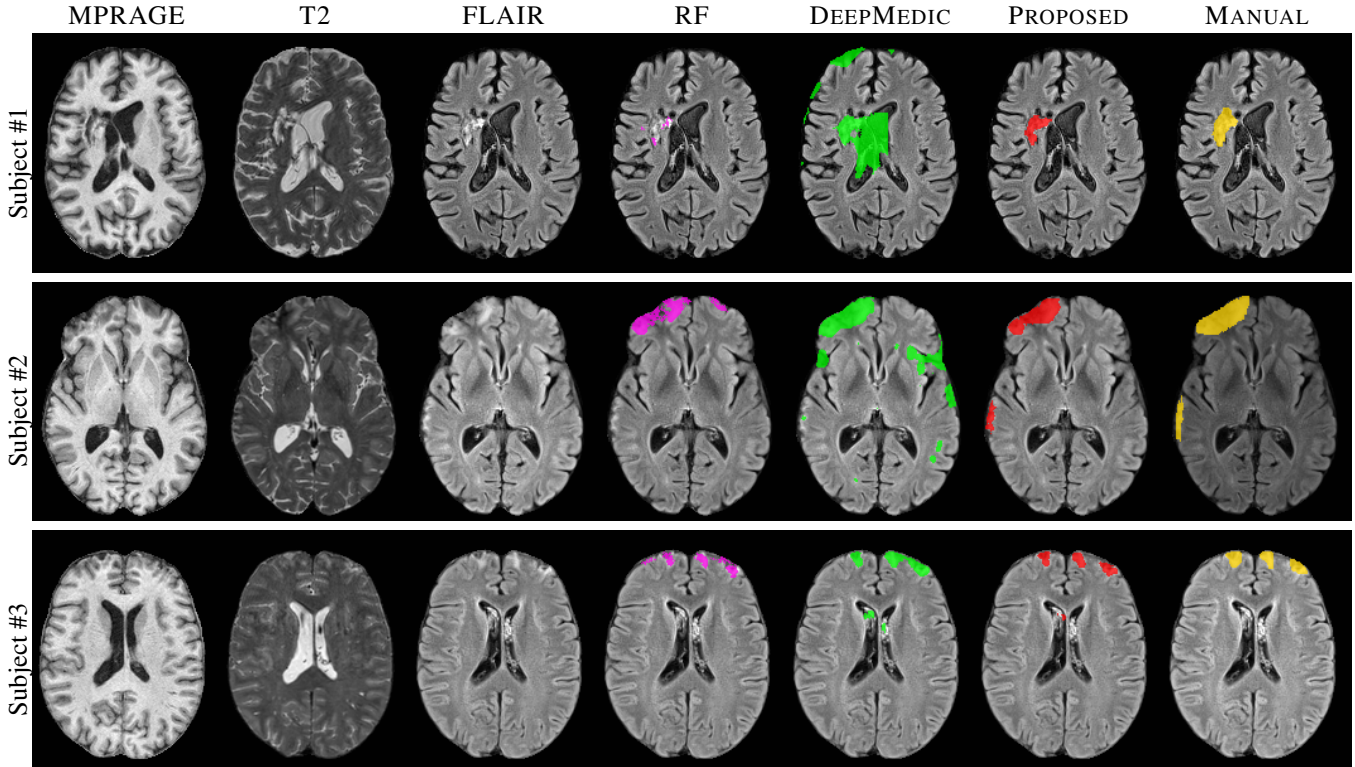


Fig. 3. Examples of segmentations are shown for 3 subjects. RF and DeepMedic corresponds to [5] and [15], respectively.

quence, the number of free parameters to estimate increases exponentially with respect to layers; for example the number of parameters in VGGNet is 140×10^6 . This can cause optimization instability when the number of training examples is many fewer than the number of free parameters. The Inception module addresses this issue by using 1×1 convolutions and having pooling and convolutions in parallel (see Fig. 2). Similar to ResNet [21], we excluded any fully connected layer.

During training, the training input consisted of mini-batches of $p \times p$ patch triplets, one for each MR contrast, from multiple atlases, where the center voxel of every patch has a non-zero label in the manual segmentations. A Gaussian blurred version of the manual segmentation, analogous to a membership, was used as the training output for estimating the parameters of the network. Therefore, for every training MR patch, instead of predicting the lesion label of the center voxel, we predict the $p \times p$ membership of the whole patch by using mean squared error as the metric. There are some advantages of using such a training procedure.

1. Since the network is fully convolutional and includes low-resolution features via average pooling instead of downsampling and upsampling, the training atlas image sizes do not need to be the same. Similarly, the testing image size also need not be the same as the training atlas sizes, as was the case in [14]. This has a practical

advantage in that the trained model can be applied to a subject image of any size without knowing the atlas dimensions.

2. The total number of parameters is only approximately 294,000, which is comparable to the number of training patches.
3. With the removal of fully connected layers and direct estimation of memberships via minimizing mean squared error, we observed that the resultant memberships were crisper, thereby producing fewer false positives than a comparable network with a fully connected layer, such as DeepMedic.

We used 45×45 patches to train the network. Since the patches were 2D, we reoriented the atlases into axial, coronal, and sagittal orientations, and trained one model for each orientation separately. Adam [22] was used to optimize the convolution filter weights via stochastic gradient descent. An average of 450,000 patches were used for training using 17 atlases, of which 20% was used for validation. Training using 17 atlases took about 10 hours for 10 epochs with a mini-batch size of 64. Although the original Inception paper [4] proposed 11 cascaded modules, limited experiments showed only 3 modules to be sufficient for an accurate segmentation. For a new subject, three memberships were generated

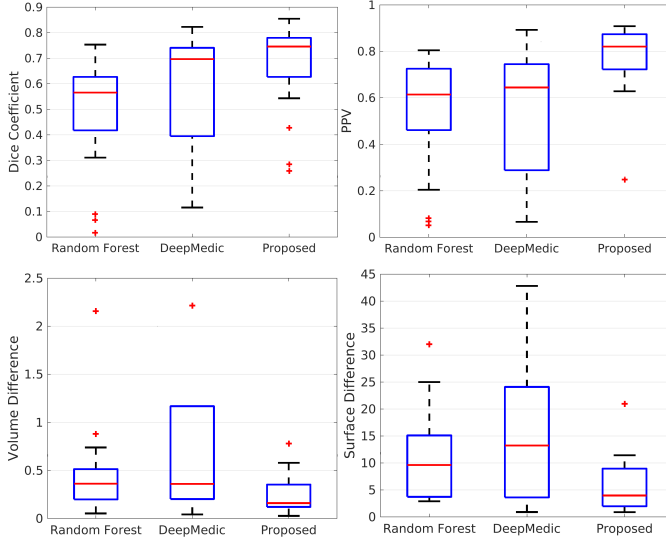


Fig. 4. Quantitative comparison between the three competing methods are shown. The proposed method shows significant ($p < 0.05$) improvement over other two methods for all four metrics.

for each orientation and then averaged to get the final membership. The memberships were thresholded at 0.5 to obtain a binary segmentation. To decrease false positives, small disconnected objects with volumes less than a certain threshold were removed from the binary segmentation. The volume threshold was computed as 90th percentile of volumes of all the 18-connected objects in a binary segmentation. Generating memberships on a new subject takes about 1 minute.

4. RESULTS

The proposed method was compared with a random forest based algorithm [5], denoted by RF and implemented in-house, as well as another CNN based algorithm DeepMedic [15]. A leave-one-out cross-validation was performed on the 18 subjects for each of the three competing methods. Example segmentations of the three methods are shown in Fig. 3 for 3 subjects. On average, RF resulted in under-segmentation and DeepMedic resulted in over-segmentation and more false positives. DeepMedic showed false positives near the right frontal lobe in subject #1 and left temporal lobe in subject #2, where there are some hyperintense artifacts on FLAIR. Neither RF nor the proposed method had any false positive around those artifacts. On subject #1, the ventricles in FLAIR were incorrectly segmented by DeepMedic. There were some CSF flow artifacts in the ventricles of subject #3, which were segmented as lesions by both DeepMedic and the proposed method.

For quantitative comparison, we used Dice coefficient, positive predictive value (PPV), volume difference (VD), and

surface difference (SD). Assuming \mathcal{A} and \mathcal{M} to be the automated and the manual binary segmentations, Dice is defined as $\frac{2|\mathcal{A} \cap \mathcal{M}|}{|\mathcal{A}| + |\mathcal{M}|}$, where $|\cdot|$ indicates number of non-zero voxels. PPV is defined as the ratio of true positives and total number of positive voxels, i.e., $\frac{2|\mathcal{A} \cap \mathcal{M}|}{|\mathcal{A}|}$. VD is defined as the ratio between absolute volume difference and manual volume $\frac{abs(|\mathcal{A}| - |\mathcal{M}|)}{|\mathcal{M}|}$. SD is defined as the average of the Hausdorff distances from \mathcal{M} to \mathcal{A} and \mathcal{A} to \mathcal{M} .

Fig. 4 shows boxplots of Dice, PPV, VD, and SD of the three methods. Median Dice coefficients for RF, DeepMedic, and our method were 0.566, 0.697, and 0.746. Median PPV values were 0.614, 0.645, and 0.821, respectively. The proposed method produced significantly higher Dice and PPV ($p < 0.01$) and lower VD and SD ($p < 0.05$) compared to the other two methods. Median VD and SD values were $\{0.362, 0.360, 0.160\}$ and $\{9.62, 13.23, 3.97\}$, respectively. DeepMedic showed higher Dice ($p = 0.005$) but similar PPV, SD, and VD compared to RF ($p > 0.25$). As observed in Fig. 3, DeepMedic had more false positives than the proposed method, evident from its high VD and low PPV. We observed that most of the false positives in our method arose from flow artifacts inside the lateral and 3rd ventricles, as shown in Fig. 3 subject #3. The false positives for RF and DeepMedic were also in the cortical region, especially in the temporal cortex, such as Fig. 3 subject #2.

5. DISCUSSION

We have described a fully convolutional neural network based algorithm to segment TBI lesions from multi-contrast MR images. Comparison with a random forest based algorithm and another CNN based algorithm on 18 subjects showed that our method produces more accurate segmentation and less false positives.

We hypothesize that the low false positive rate in our proposed method was attributed to bigger patch sizes (45^2 vs 17^3 in DeepMedic) and removal of fully connected layers. Bigger patches provide more context to a lesion, thereby reducing the risk of false positives. This is seen in Fig. 3 subject #3, where the false positives inside the ventricles was reduced in the proposed method.

We have used 2D patches separately in three orientations to train three models. The rationale behind using 2D patches is that the FLAIR images, which usually produce the best contrast for lesions, are anisotropic ($1 \times 1 \times 3$ mm³) in resolution. So a full isotropic patch may include spurious or irrelevant information regarding a small lesion. Also by using 2D models, we were able to use large (4.5×4.5 cm) patches which include more context to a small region of interest, while fitting within a small GPU memory. Future work will include optimization of the patch size and the depth of the network, comparison with full 3D patches, and differentiating types of lesions.

6. REFERENCES

- [1] K. M. Kinnunen and *et. al.*, “White matter damage and cognitive impairment after traumatic brain injury,” *Brain*, vol. 134, no. 2, pp. 449–463, 2011.
- [2] G. Trifan, R. Gattub, E. M. Haacke, Z. Kou, and R. R. Benson, “MR imaging findings in mild traumatic brain injury with persistent neurological impairment,” *Mag. Reson. Imaging*, vol. 37, pp. 243–251, 2017.
- [3] K. G. Moen, T. Skandsen, M. Folvik, V. Brezova, K. Arne Kvistad, J. Rydland, G. T Manley, and A. Vik, “A longitudinal MRI study of traumatic axonal injury in patients with moderate and severe traumatic brain injury,” *J. of Neurology, Neurosurgery & Psychiatry*, vol. 83, no. 12, pp. 1193–1200, 2012.
- [4] C. Szegedy and *et. al.*, “Going deeper with convolutions,” in *Intl. Conf. on Comp. Vision. and Patt. Recog. (CVPR)*, 2015, pp. 1–9.
- [5] D. Zikic, B. Glocker, E. Konukoglu, A. Criminisi, C. Demiralp, J. Shotton, O. M. Thomas, T. Das, R. Jen, and S. J. Price, “Decision forests for tissue-specific segmentation of high-grade gliomas in multi-channel MR,” in *Med. Image Comp. and Comp. Asst. Intervention (MICCAI)*, 2012, vol. 7512, pp. 369–376.
- [6] A. Rao, C. Ledig, V. Newcombe, D. Menon, and D. Rueckert, “Contusion segmentation from subjects with traumatic brain injury: A random forest framework,” in *Intl. Symp. on Biomed. Imag. (ISBI)*, 2014, pp. 333–336.
- [7] A. J. Asman, L. B. Chambless, R. C. Thompson, and B. A. Landman, “Out-of-atlas likelihood estimation using multi-atlas segmentation,” *Medical Physics*, vol. 40, no. 4, pp. 043702, 2013.
- [8] C. Ledig, R. A. Heckemann, A. Hammers, J. C. Lopez, V. F. J. Newcombe, A. Makropoulos, J. Lotjonen, D. K. Menon, and D. Rueckert, “Robust whole-brain segmentation: Application to traumatic brain injury,” *Med. Image Anal.*, vol. 21, pp. 40–58, 2015.
- [9] S. Roy, Q. He, E. Sweeney, A. Carass, D. S. Reich, J. L. Prince, and D. L. Pham, “Subject specific sparse dictionary learning for atlas based brain MRI segmentation,” *IEEE J. of Biomed. and Health Informatics*, vol. 19, no. 5, pp. 1598–1609, 2015.
- [10] S. Roy, A. Jog, A. Carass, and J. L. Prince, “Atlas based intensity transformation of brain MR images,” in *Intl. Workshop on Multimodal Brain Image Analysis (MBIA)*, 2013, pp. 51–62.
- [11] Y. LeCun, Y. Bengio, and G. Hinton, “Deep learning,” *Nature*, vol. 521, no. 7553, pp. 436–444, 2015.
- [12] B. H. Menze and *et. al.*, “The multimodal brain tumor image segmentation benchmark (BRATS),” *IEEE Trans. Med. Imag.*, vol. 34, no. 10, pp. 1993–2024, 2014.
- [13] M. Havaei, A. Davy, D. Warde-Farley, A. Biard, A. Courville, Y. Bengio, C. Pal, P.-M. Jodoin, and H. Larochelle, “Brain tumor segmentation with deep neural networks,” *Med. Image Anal.*, vol. 35, pp. 1831, 2017.
- [14] Olaf Ronneberger, Philipp Fischer, and Thomas Brox, “U-net: Convolutional networks for biomedical image segmentation,” in *Med. Image Comp. and Comp. Asst. Intervention (MICCAI)*, 2015, vol. 9351, pp. 231–241.
- [15] K. Kamnitsas, C. Ledig, V. F. J. Newcombe, J. P. Simpson, A. D. Kane, D. K. Menon, D. Rueckert, and B. Glocker, “Efficient multi-scale 3D CNN with fully connected CRF for accurate brain lesion segmentation,” *Med. Image Anal.*, vol. 36, pp. 61–78, 2017.
- [16] B. B. Avants and *et. al.*, “A reproducible evaluation of ANTs similarity metric performance in brain image registration,” *NeuroImage*, vol. 54, no. 3, pp. 2033–2044, 2011.
- [17] S. Roy, J. A. Butman, D. L. Pham, and Alzheimers Disease Neuroimaging Initiative, “Robust skull stripping using multiple MR image contrasts insensitive to pathology,” *NeuroImage*, vol. 146, pp. 132–147, 2017.
- [18] N. J. Tustison and *et. al.*, “N4ITK: improved N3 bias correction,” *IEEE Trans. Med. Imag.*, vol. 29, no. 6, pp. 1310–1320, 2010.
- [19] M. D. Zeiler and R. Fergus, “Visualizing and understanding convolutional networks,” in *European Conf. on Comp. Vision (ECCV)*, 2014, vol. 8689, pp. 818–833.
- [20] K. Simonyan and A. Zisserman, “Very deep convolutional networks for large-scale image recognition,” in *arXiv preprint arXiv:1409.1556*, 2014.
- [21] K. He, X. Zhang, S. Ren, and J. Sun, “Visualizing and understanding convolutional networks,” in *Intl. Conf. on Comp. Vision. and Patt. Recog. (CVPR)*, 2016, pp. 770–778.
- [22] D. P. Kingma and J. Ba, “Adam: A method for stochastic optimization,” in *Intl. Conf. on Learning Representations (ICLR)*, 2015.